

## **Copepods size structure in various phases of a cold-core eddy - Normalised Abundance Size Spectra (NASS) approach.**

**<sup>1</sup>L. Jagadeesan\*, <sup>1</sup>T.N.R. Srinivas, <sup>1</sup>A. Surendra, <sup>1</sup>G.Sampath Kumar, <sup>2</sup>Aswin Dev and <sup>2</sup>Ignatious Joseph**

<sup>1</sup>CSIR-National Institute of Oceanography, Regional Centre, Visakhapatnam, India

<sup>2</sup>School of Ocean Science and Technology, Kerala University of Fisheries and Ocean Studies, Panangad, India

\* Corresponding author, E-mail: jagadeesanl@nio.org

### **Abstract**

The present study addresses the copepods size structure in different phases of a cold-core eddy based on a 17 day time-series measurement (21<sup>st</sup> February to 8<sup>th</sup> March 2016) from a coastal site in the western Bay of Bengal during the Spring Intermonsoon (SIM). Copepod size measured using FlowCAM and microscope was converted into biovolumes. Based on the salinity and temperature in discrete depth layers, sampling days were grouped into 3 Phases, pre-eddy (21- 24 February), Core-eddy (28 February – 6 March) and transition (25 - 27 February and 7 - 8 March). The core-eddy phase was characterised as cool, less oxygenated and nutrient-rich in subsurface layers than pre-eddy and transition. Copepod abundance and total biovolume were relatively high in core-eddy phase compared to other phases. Copepods biovolumes were arranged in 15 size classes. Contribution of each size classes in total biovolume differed between the eddy phases. In total biovolume, smaller copepods (biovolume size class  $\leq \log_2(-3) \text{ mm}^{-3}$ ) contribution was high (76.84%) in pre-eddy, but larger copepods proportion was high in core-eddy phase. Normalised Abundance Size Spectra (NASS) slope varied from -2.45 to -1.02. Similar to the taxonomic diversity, size diversity also high in core-eddy phase. Relatively flatter slope, high intercept and diversity in core-eddy phase suggest that copepods production and trophic efficiency was substantially increased. In short, copepods taxonomy and their size structure explain, pre-eddy contains the smaller coastal forms and core-eddy have a mixture of smaller coastal, larger oceanic and Oxygen Minimum Zone (OMZ) tolerant forms. Larger oceanic and OMZ tolerant forms in core-eddy phase indicate their entry through the transverse of the offshore formed cold-core eddy in the study site. Slope, intercept of NASS and size diversity captured the copepod species composition and production differences between the eddy phases in terms of abundance. This study suggests plankton size spectra and size diversity can be used as a tool to predict the plankton food web response in the varying environmental conditions. This study is the first of its kind explaining about copepods size structure and size spectrum changes with the hydrographical characteristics in Indian waters.

**Keywords:** Copepods, Eddy time series, Size structure, Normalised Abundance Size spectra, FlowCAM.

## 1.0 Introduction

Size of an organism is one of the key factor for determining the flow of energy pattern, species diversity, community structure, in the plankton food web (Zhou and Huntley, 1997; Ke et al., 2018). Ecological modeling and management plan studies require high-resolution data sets to understand the factors that drive the shift in community structure changes and species succession (Taucher et al., 2017). Taxonomic studies comprise the large data sets in the form of abundance, species composition, community structure, species diversity. However, the inclusion of all the taxonomic information was not feasible in ecological models (Zhou and Huntley, 1997), since taxonomy studies are time-consuming and delicate (Taucher et al., 2017). Physiology of organisms mainly depended on its size (Bruce et al., 2006; Taucher et al., 2017), so size related data sets can be used to address the ecosystem changes. Size based approach is a non-taxonomic method to study planktonic organisms in a pelagic ecosystem.

Normalised Abundance Size Spectrum (NASS) useful tool summarise and elucidate particle size structure in various oceanic regions (Zhou et al., 2009; Ke et al., 2018). NASS explains abundance and size relationships in a mathematical way (Sheldon et al., 1972). In this approach, total abundance of organisms is binned size classes on an octave scale divided by the width of the size classes and plotted against size in log-log scale (Sheldon et al., 1972; Blanco et al., 1994). The slopes and intercepts used to track changes in growth, trophic structure and succession of organisms with surrounding hydrography (Zhou, 2006).

Copepods are the dominant member of the zooplankton group that plays a significant role in carbon flow between phytoplankton and higher trophic levels (Jagadeesan et al., 2013). The zooplankton growth, feeding, reproduction and metabolic rates depended upon the size (Zhou and Huntley, 1997; Taucher et al., 2017). Zooplankton size influences the phytoplankton productivity, predator abundance and fishery potential in an aquatic ecosystem (Sheldon et al., 1972; Zhou, 2006). Traditionally, the plankton food web components were quantified based on their abundance than the size (Madhupratap et al., 1996; Madhupratap et al., 2001; Rakesh et al., 2006; Fernandes, 2008; Rakesh et al., 2008; Jyothibabu et al., 2008a; Fernandes and Ramaiah, 2009; Jagadeesan et al., 2013; Jagadeesan et al., 2017a) because of the difficulties in measuring the size in a large number of samples.

Recent advancement of image-based technologies with machine learning algorithms has emerged as a useful tool for acquiring size related data on planktonic organisms in automated or semi-automated instruments like the FlowCAM, Zooscan, etc., (Alvarez et al., 2011; Wong et al.,

2017). This computer-based instruments routinely measures the size and other properties of the organisms. The application of FlowCAM has recently increased for the quantification of zooplankton (copepods) community structure and their sizes (Le bourg et al., 2015; Wong et al., 2017; Jagadeesan et al., 2017b). In FlowCAM, samples are passed through the rectangular flow cell, where the particles in the samples are captured as images by the digital camera with various size-related properties (Sieracki et al., 1998). Recent days, size-based approaches are getting more attention due to their simple nature and their possible inclusion in environmental prediction studies.

Eddies are isolated environments and sustaining unique hydrographical and biological properties from their adjacent water bodies. The Bay of Bengal was less productive compared to the eastern Arabian Sea due to stratification, warmer, low salinity, weaker winds and sporadic upwelling in the narrow band (Prasanna Kumar et al., 2002; Prasanna Kumar et al., 2004). Eddies influence the primary and secondary productivity pattern of the Bay of Bengal. Zooplankton composition and copepod species community structure differed between eddy influenced conditions compared to surroundings (Mackas et al., 2005); Eddy associated hydrography altering the trophic efficiency and plankton food web structure (Zhou et al., 2009; Zhou et al., 2015).

Size structure measurements of the copepods are the crucial element to study the ecosystem dynamics, stability, productivity and nutrients cycling. The NASS is a useful tool to track the alterations in the production and copepod community structure related to the surrounding conditions (Zhou et al., 2015). A comprehensive study involving the size, taxonomy and food web structure is considered to be the best way of explaining the trophic connectivity of an ecosystem. However, the best of our knowledge, copepod size-related quantification with NASS size spectrum approach in various phases of eddy conditions are absent in Indian waters.

We hypothesize that the copepod community size structure significantly different in an eddy environment. In order to verify that, copepods size structure was measured at a coastal location through which a cold-core eddy was moving. 17-day time-series sampling was conducted from the study site during the SIM period to cover various phases of eddy (Figure 1) in the Western Bay of Bengal (BoB). The main objective of the present study was to quantify the copepods size structure during the various phases of a cold-core eddy. The first part of this work explaining changes in the zooplankton composition and copepods community structure related to the hydrography alteration caused by a moving cold core eddy is already published (Jagadeesan et al., 2019). This present manuscript mainly focuses on the copepods size structure changes in various eddy phases. Further, this study examined the appropriateness of the size based measurements for future prediction studies

through comparison of the size diversity, NASS details with the taxonomic diversity and community structure.

## **2.0 Material and methods**

Onboard time-series study was conducted in off Bheemunipatnam (18°N; 84°E) (Figure 1) during 21<sup>st</sup> February to 8<sup>th</sup> March 2016. Geostrophic currents were downloaded from <http://marine.copernicus.eu/> and plotted in Ocean data view software to represents the eddy phases. Vertical profiles of the temperature and salinity measured at short term intervals (1 hrs intervals) using rosette CTD. For measure the dissolved oxygen, nutrients and pigments, samples were collected in every 3 hrs from 8 depth layers. Dissolved oxygen concentrations measured in Winkler's method and nutrients measured using the standard procedure of Grasshoff et al., 1983. 5-10 L of the water samples were filtered in 0.2 µm filters papers and extracted with 3ml of 90% acetone for quantifying the concentration of the pigments in HPLC (Agilent Technology; Series 1200). CTD measured Chlorophyll *a* was corrected with the lab measured Chlorophyll *a* ( $1.263 * \text{CTD Chl. } a + 0.075$ ;  $r=0.94$ ;  $P<0.0001$ ) for representing the vertical profile and integrated Chl.*a* analysis.

Mesozooplankton samples were collected through vertical hauls (100 m to the surface) of WP-2 net (mouth diameter- 50cm; mesh size 200µm) in every 6 hrs. Digital flowmeter (Hydrobioas) was died across the net rings to calculate the volume of water passed through the net. Collected net samples were preserved in the 5% formalin for further analysis. 25-50% of the subsample in each net collection was separated into several groups and quantified (Postel et al. 2000). Among the various groups, copepods were identified into species level with the help of the standard keys (Kasturirangan, 1963; Conway et al., 2003; <https://copepodes.obs-banyuls.fr/en/index.php>). In the sorted copepods, 6 AM sample in each day used in size structure measurements. The dominant species in various phases of the eddy was analysed using the dominance index analysis (Yang et al., 1999). Multivariate hierarchical Cluster/ multidimensional scaling (NMDS) analysis with Similarity Profiles (SIMPROF) permutation analysis were carried out for grouping the observational days in a statistically significant way ( $P<0.05$  significance level) (Clarke and Gorley, 2006), based on the relatedness in the salinity and temperature in discrete depth layers (10m, 15m, 20m, 25m, 30m, 35m, 40m, and 50m). Cluster and NMDS analysis were performed using PRIMER V6 software package.

### **2.1. Copepods size, biovolume measurements and biomass conversion**

The FlowCAM used in this study was a basic Model with visual spreadsheet V4. This basic FlowCAM model can able to capture the particles sizes ranged from 3 to 3000 µm using various magnifications and Flowcell combinations. For effective and routine copepods size measurements in

FlowCAM, copepods samples are initially separated into various size classes like large (>1000 µm), medium (500-1000 µm) and small (200 - <500 µm) by sieving through 1000µm, 500µm and 200µm micron meshes. The small and medium-sized copepods were separately analysed in FlowCAM using auto image mode, frame rates of 9 using 2 X 2 mm flow cell (Field of View) in the combination of 2x magnification. For avoiding clogging and effective imaging and proper size measurement, the larger copepod fractions analysed in the microscope. The repeated images and partial images omitted in biovolume calculations in FlowCAM samples. ABD (Area based diameter) diameter and ABD biovolume of copepods used for size structure and size spectrum analysis. Larger copepods body measurements measured using microscopes and copepods biovolume is calculated using the standard formula of the Viñas et al., 2010.

$$V = 1/6\pi (P_L * P_W * P_H) + 1/4 \pi (U_L * U_{W1} * U_{W2})$$

Where, V= Biovolume; P<sub>L</sub> – Prosome length; P<sub>W</sub>- Prosome width; P<sub>H</sub>- Prosome height; U<sub>L</sub> – Urosome length, U<sub>W1</sub>- Urosome width<sub>1</sub> (widest portion) and U<sub>W2</sub> – Urosome width<sub>2</sub> (width of the narrower portion). The measurements of the length, width and height according to Viñas et al., 2010. FlowCAM and microscope measured sizes were pooled together for assessing the copepods community size structure.

## 2.2 Normalised abundance size spectrum (NASS)

For obtaining the abundance size spectra, based on the size copepods abundance were distributed into 15 biovolume classes (mm<sup>-3</sup>) on an octave scale. Total abundance of copepods in each biovolume size classes divided by the width of the size class for normalisation. Normalised abundance and their biovolume size classes are plotted on the log-log scale and fitted with a linear regression model to estimate slopes and intercepts of the biovolume abundance spectra (Ke et al., 2018).

$$\log_2 (A_i / \Delta V) = a \log_2 v_i + b$$

A<sub>i</sub> is total copepods abundance in the size class; v<sub>i</sub> is the lower limit of the biovolume class; ΔV is the width of the size class (upper values minus lower values); b – Intercept and a slope.

## 2.3 Taxonomic and size diversity

Taxonomic and size diversity of the copepods was calculated by the Shannon Weaver index formula

H' = - Sum pi log<sub>2</sub>pi (Shannon and Weaver, 1963). In taxonomic diversity, pi is the proportions of

species  $i$  relation to its total abundances; while in size diversity,  $p_i$  is the proportion of the size class  $i$  in relation to the total biovolume.

## **2.4 Univariate and multivariate analysis**

Temporal differences of the hydrographical and biological parameters between the eddy phases analysed using One-way ANOVA. ANOVA was performed as per the standard procedure of Zar, (1999) using XL stat pro- software package. Multivariate analysis was conducted to find the relationships between hydrographical parameters and copepods abundance, total biovolume and proportions of various sizes in total biovolume and NASS slopes in different eddy phases. Initially, Detrended correspondence analysis (DCA) was performed to select the correct ordination methods for the present study (Leps and Smilauer, 2003). The results of the DCA shows that the length of the axis was  $<2$ ; this suggests RDA is the proper ordination pattern to explain the interrelationships between the parameters in the present data sets. The outcome of the RDA was presented in the form of Triplot. The total copepods abundance and total biovolume were log-transformed before the RDA and significance of the RDA tested with Mote-Carlo test (Leps and Smilauer, 2003). DCA and RDA performed in CANOCA software version 4.5.

## **3.0 Results**

### **3.1 Cold-core eddy movements**

One moving cold-core eddy was found  $\sim 1^\circ$  south from the study location during the first week of February and it slowly moving towards north along with East India Coastal Current (EICC) (Supplementary Figure 1). SSHA was positive in first week February, later it changing towards negative (Supplementary Figure 1). The study location faced the closeness of core eddy during the second week of February. Core eddy was in the study site during the fourth week of February to March first week (01-06 March), later the period, eddy core moved out from the study location. The course of this eddy transverse, we tracked the various eddy phases in the study site.

### **3.2 Grouping of sampling days based on the vertical pattern of the salinity and temperature**

Vertical pattern of the salinity and temperature differed significantly between the sampling days. Up slopping of  $>34$  psu salinity (high saline) and  $25^\circ\text{C}$  temperature (cool) in subsurface water ( $\sim 45\text{m}$  to  $30\text{m}$ ) was evident during the fourth week of February to 1<sup>st</sup> week March (Figure 2). Based on the Sea surface height anomaly, temperature and salinity in discrete depth layers, cluster/SIMPROF analysis separated the sampling periods into three phases (Figure 3). Phase – I represents the pre-eddy (21 -24 February) characterised by a relatively warm, less saline in subsurface water. Phase II represents the core-eddy (28 February - 06 March) characterised by

relatively cool and high saline in subsurface layers. Intermittent conditions of the between the pre-eddy and core-eddy considered as the Phase III/ transition phase (25 - 27 February and 7-8 March) (Figure 2 and 3).

### 3.3 Dissolved oxygen, nutrients and Chlorophyll-*a*

Dissolved oxygen remains saturated in surface layers during the entire sampling period. In the subsurface layer, dissolved oxygen variations between the phase of eddy were significant (ANOVA,  $P < 0.05$  – Supplementary Table 1). DO was relatively high ( $0.83 \text{ mg. L}^{-1}$  in 75m,  $0.51 \text{ mg. L}^{-1}$  in 100m) in pre-eddy; it decreased almost half ( $0.42 \text{ mg. L}^{-1}$  in 75m,  $0.28 \text{ mg. L}^{-1}$  in 100m) during core-eddy phase (Table 1). Nutrient levels in the surface were uniformly low, but in the subsurface layer (20-50m), nutrient concentrations increased 0.5 to 1 fold high during core-eddy phase (Table 1). Chlorophyll *a* was ranged between 0.2 and  $0.45 \mu\text{g. L}^{-1}$  in the surface layer. Temporal variation of the Chlorophyll *a* in the surface layer was comparable (Supplementary Table 1). Subsurface Chlorophyll *a* Maxima (DCM) was in 38 m during the phase I and it up sloped to 23m in core-eddy phase, 32m in the periphery condition (Figure 4). The integrated Chlorophyll *a* (0-100m) was high during transition compared to the other two phases.

### 3.4 Copepods abundance, community structure and diversity

Copepods abundance (0-100m) ranged between 30097 and 70559  $\text{No.m}^{-2}$  during the entire study period. Copepod abundance ( $\text{No.m}^{-2}$ ) was less in pre-eddy ( $37919 \pm 3642$ ) compared to core-eddy ( $55592 \pm 6570$ ) and transition ( $38719 \pm 5554$ ) (Figure 5a). Sixty-four copepod species were identified, in that 14 found as dominant species. Out of 14 species, seven species found as common dominant forms in all three phases (Table 2). *Temora turbinata* (upwelling indicator), *Pleuromamma indica* (Oxygen Minimum Zones - OMZ tolerant and indicator), *Canthocalanus pauper*, *Undinula vulgaris*, *Pseudodiaptomus serricaudatus* dominance found in core-eddy phase in addition to the common dominant forms. *Pleuromamma indica* abundance was specifically high in core-eddy. In addition to the *Pleuromamma indica*, other 11 offshore and OMZ reported copepods appearance reported during the core-eddy phase (more details, please see Jagadeesan et al., 2019). The proportions of copepods species in total abundance differed between eddy phases. Poecilostomatoida (presently included within cyclopoida) dominated during pre-eddy, while calanoids dominated during the core-eddy (Figure 5b).

### 3.5 Size structure and total biovolume of copepods

Copepods individual biovolume was ranged from  $0.03 \text{ mm}^{-3}$  to  $1.986 \text{ mm}^{-3}$ . As like the compositional differences copepods community size structure also significantly varied between

phases (ANOVA, F ratio = 6.63; P<0.05). Integrated total copepods biovolume was less during pre-eddy ( $2294 \pm 526 \text{ mm}^{-3}$ ), moderate during the transition ( $3791 \pm 1702 \text{ mm}^{-3}$ ) and high during core-eddy phase ( $5986 \pm 2406 \text{ mm}^{-3}$ ) (Figure 6). Dominant species mean biovolume in various eddy phases was presented in Table 3. Based on the biovolume, dominant copepods are in the order of *Corycaeus danae* < *Farranula gibbula* < *Oncaea venusta* < *Euterpina acutifrons* < *Acrocalanulus* sp., < *Calocalanus pavo* < *Paracalanus parvus* < *Canthocalanus pauper* < *Centropages calaninus* < *Temora turbinata* < *Pseudodiaptomus serricaudatus* < *Undinula vulgaris* < *Eucalanus elongatus* < *Pleuromamma indica*. Copepods biovolume in binned size classes showed smaller portions (biovolume size class  $\leq \log_2(-3) \text{ mm}^{-3}$ ) dominated (76.8%) in total biovolume during the pre-eddy, which transformed into larger copepods (63%) during the core-eddy. In larger copepods, biovolume was 2-10 folds high in core-eddy than pre-eddy (Figure 6b).

### 3.6 Normalised abundance size spectrum of copepods

Slopes and intercepts of the NASS during the sampling periods were presented in Table 4. NASS slopes were varied from -2.45 to -1.02 during the study period. The negative relationship between the size intervals and abundance indicates the copepods abundance was decreased towards the larger size classes (Figure 7). The slope differences between the eddy phases are significant (ANOVA, DF=2, N=17, F ratio = 23.48; P<0.001). NASS slope is steeper in pre-eddy phase (-1.95) and relatively shallower in the periphery (-1.52) and core-eddy (-1.20) (Figure 7). Intercept values of the NASS spectrum were relatively high in the core-eddy (8.08) compared to pre-eddy (4.60) and transition (6.49) (Figure 7).

### 3.7 Taxonomic and size diversity of copepods

Copepods species diversity varied between 2.47 and 2.95, and size diversity varied from 2.2 to 2.60. Size diversity and species diversity differences were significant between the phases (Figure 8). Size and taxonomic diversity was high in core-eddy phase (taxonomic diversity:  $2.89 \pm 0.20$ ; Size diversity:  $2.45 \pm 0.12$ ) compared to pre eddy (taxonomic diversity:  $2.48 \pm 0.24$ ; size diversity:  $2.24 \pm 0.07$ ) and transition phase (taxonomic diversity:  $2.69 \pm 0.15$ ; size diversity:  $2.37 \pm 0.11$ ).

### 3.8 Relationships between environmental parameters and copepods size distribution

RDA triplot explains the distribution as well as interrelationships of the environmental parameters and biological parameters (Figure 9). Altogether environmental parameters explained the 83.5 % variance of the biological parameters (Copepods abundance, total biovolume, contributions of the various copepods in biovolume and NASS spectrum of copepods community size structure). The results of the Monte Carlo permutation test explains the represented triplot pattern was



statistically significant ( $F=23.63$ ;  $P=0.0020$ ). The environmental axes distribution clearly visualises temporal differences of the hydrographical parameters between the three different phases. The increasing direction of the subsurface temperature, dissolved oxygen and SSHA along with Phase I (pre-eddy) sampling days (right-hand side of the RDA) represents that pre-eddy has comparatively oxygen-rich and warmer. The positive direction of the salinity and nutrients with the core-eddy sampling days represents that (Figure 9) core-eddy characterised as relatively saltier, cool and nutrient rich. Transition phase condition was between the core-eddy and pre-eddy. Copepod abundance and dominant species axes pattern explain their distribution differed between the eddy phases. Copepod abundance axis orientation positive direction with salinity and negative direction to temperature along with the observations of the core-eddy phases indicates their high abundance in core-eddy (Figure 9). Total biovolume oriented with a similar direction of copepods abundance indicates the core-eddy has higher copepods biomass than the other two phases. The contribution of the size fractions in the total biovolume differed between the eddy phases was evident in the orientation pattern of the smaller and larger copepods axes. Smaller copepods proportions and the Poecilostomatoids copepods contribution in total abundance axes were oriented towards the pre eddy hydrographical characteristics and observations represent the smaller copepods were high in pre eddy. Larger copepod proportions and calanoids copepods axes towards the left-hand side of the plot represent that relatively larger calanoids copepods were high in the core-eddy. Normalised Abundance Size Spectrum slope positive with the core-eddy characteristics represents the NASS was steeper in the pre eddy and flatter in the core-eddy. The slopes of NASS, individual copepods biovolume of the dominant species, total biovolume in different size classes, contribution of the copepods orders in total abundance together represents that smaller coastal copepods dominate in the pre-eddy; core-eddy has the mixture of small and large copepods (coastal and oceanic).

#### **4.0 Discussion**

Eddies are the consistent mesoscale feature in the Bay of Bengal (Jyothibabu et al., 2015). EICC flow direction towards equatorward during the winter monsoon period and poleward during the Spring Intermonsoon period (Shetye et al., 1993, 1996; Shankar et al., 2002). One cold-core eddy found  $\sim 1^\circ$  south from the study site during the first week of February, and it moves slowly towards north along with the flow of EICC, in this course of movement eddy passed via the study site. The entire observational days were divided into three conditions Viz., pre-eddy, core- eddy and transition based on changes in the hydrographical characteristics in the water column due to passage of the eddy. In overall, hydrographical parameters variations in the surface layer was comparable between the sampling days. However, upward movement of cool, nutrient-rich and less oxygenated waters

found in subsurface layers during the eddy conditions. The surface salinity stratification inhibits the cold core eddy pumping to reaches the surface in the Bay of Bengal ( Prasanna Kumar et al., 2007; Sarma et al., 2018) this was in agreement with the vertical pattern of the salinity and temperature of the present study. Comparatively shallow subsurface Chlorophyll a (DCM) layer during core-eddy compared to pre eddy conditions indicates the eddy pumped nutrients enhanced productivity in euphotic layers (Prasanna Kumar et al., 2004; Madhu et al., 2006; Jyothibabu et al., 2008b; Mahadevan, 2014).

Copepods total abundance was significantly high in the cold-core compared to other phases, in accordance with previous studies (Fernandes, 2008; Fernandes and Ramaiah, 2009). Copepods growth, reproduction, size and species succession in an environment was influenced by the quality, preferences and availability of food with the prevailing environmental condition (Anjusha et al., 2013; Jagadeesan et al., 2017b). Poecilostomatoids (*Oncaea* and *Corycaeus danae*) are dominant over calanoids *during* the pre-eddy condition. Pre-eddy represents the Spring Intermonsoon condition of the Bay of Bengal. During SIM, BoB characterized as nutrient less and low productive (Jyothibabu et al., 2008b). However the abundance of microbial food web components were high (Jyothibabu et al., 2008b). Availability of food in surroundings and food preferences of copepods alters the copepods community structure. Availability of high microbial food components and relatively less phytoplankton would be the reason for the high abundances of the carnivorous Poecilostomatids (Wu et al., 2004) during the Pre-eddy period. Irrespective of the eddy phases, *Acrocalanus*, *Paracalanus parvus*, *Calocalanus pavo*, *Eucalanus elongates*, *Centropages calaninus* was reported as the dominant forms; but their biovolume and abundance were relatively high in the core-eddy compared to pre eddy. The laboratory feeding experimental studies show that dominant calanoids copepods are herbivorous or omnivorous; they ingest both the phytoplankton and microzooplankton but their favourite choice towards phytoplankton. Poecilostomatids are Reasonably high carbon intake utilise for growth and production, this could be the reason for their high biovolume and more abundance in core-eddy phase. The high abundance of opportunistic species such as *Temora turbinata* and *Pseudodiaptomus serricaudatus* utilised the phytoplankton and increased their size and abundance (Madhupratap et al., 1992; Jagadeesan et al., 2013). *Canthocalanus pauper*, *Pleuromamma indica*, *Undinula vulgaris* and the other several offshore and OMZ abundant forms found in core-eddy conditions. Larger oceanic and OMZ tolerant forms in core-eddy indicate their entry through the transverse of the offshore formed cold-core eddy in the study site (Jagadeesan et al., 2019).

Size structure can provide crucial information about organism's metabolism, food selection and trophic role of organisms in the food web (Gillooly et al., 2001; Bruce et al., 2006; Woodward et al., 2005; Visser and Fiksen, 2013). Copepods species composition and their size structure differed between the non-eddy and eddy conditions. Total copepods biovolume (0-100m) significantly differed between the eddy phases (ANOVA,  $P < 0.05$ ) with a high total biovolume in the core-eddy followed by the transition and least during the pre-eddy. Smaller copepods (BV size class  $\leq \log_2 -2 \text{ mm}^3$ ) contribution was high in pre-eddy (76.84%) and larger size classes dominated during core-eddy associated with the abundance of offshore organisms, phytoplankton productivity, feeding preferences and surrounding hydrography.

Biovolume abundance size spectra related the total biovolume of organisms of a certain size to its size class (Sheldon et al. 1972). NASS slopes speculate the metabolic capabilities of an organism such as respiration, growth, survival and mortality even without the detailed taxonomic studies (Platt, 1978; Silvert and Platt, 1978; Zhou, 2006). The size spectrum combined with environmental data can furnish the factors controlling their distribution (Zhou, 2006). The slopes of the size spectrum and size diversity can be used as an index to represent the pattern of energy flow either from bottom-up or top-down control of the marine ecosystem (Ye et al., 2013; Zhou, 2006). Copepods species and size diversity were high in core-eddy compared to non-eddy, related to the occurrences of offshore forms, OMZ tolerance forms and proliferation of the opportunistic species in core-eddy phase.

An increase in the size diversity can accelerate the top-down control on phytoplankton through diet partitioning (Ye et al., 2013; Marcolin et al., 2013). NASS slopes significantly differed between eddy phases. The slope of NASS was shallow during the core-eddy (-1.20) as compared to pre eddy (-1.95) and transition phases (-1.52). Intercept obtained from the size spectrum of zooplankton community structure reflects the production (Ke et al., 2018). The high intercept indicates a high copepods production in core-eddy (8.08) compared to Pre eddy (4.6) and transition (6.49) phases, which was consistent with the copepods abundance and total biovolume.

Relatively steeper slope, lesser biovolume, lowest diversity along with the less phytoplankton is the indication of the minimal transfer (phytoplankton to copepod) efficiency (Ye et al., 2013; Marcolin et al., 2013) during Spring Intermonsoon. This was in agreement with the earlier observation of Gauns et al., (2005); Madhu et al., (2006); Jyothibabu et al., (2008b) about the least phytoplankton production during SIM and the importance of microzooplankton in plankton food web dynamics of BoB. Relatively flatter slopes, high biovolume, higher size diversity, with the high phytoplankton are an indication of high transfer efficiency (phytoplankton to copepod) during the

core-eddy. NASS and size diversity captured the variations of the copepods community and production differences in terms of abundance and trophical positioning. So, this study supports the view of plankton size spectra can be used efficient tool to predict the response of plankton food web response in variations in the environmental conditions. This study is the first comparative study to report the size distribution of copepods with NASS in various eddy phases through time-series studies.

## 5. Conclusion

. Seventeen days' time-series measurements were carried out to study the copepods community size structure in various phases of a cold-core eddy in the western Bay of Bengal during the SIM (21<sup>st</sup> February to 8<sup>th</sup> March 2016). Sampling days were grouped into 3 clusters based on the SSHA, salinity, temperature distribution in subsurface layers such as cluster I or pre-eddy (21<sup>st</sup> - 24<sup>th</sup> February), cluster II or core-eddy (28<sup>th</sup> February - 6<sup>th</sup> March) and phase III (transition/periphery – 25<sup>th</sup> to 27<sup>th</sup> Feb and 7<sup>th</sup> March - 8<sup>th</sup> March ). The pre-eddy was typical of the spring intermonsoon characterised by relatively low saline, warmer and more oxygenated in subsurface waters. Core-eddy phase was cool, less oxygenated and nutrient-rich in subsurface layers. Transition was intermediate between these two phases. Copepods abundance was high during core-eddy compared to the other two phases. Total biovolume was high in core-eddy phase than the pre-eddy and transition. Total copepods biovolume in each size classes differed between the eddy phases. The entire copepods biovolume arranged into 15 size classes intervals. During Pre eddy, smaller copepods (biovolume size class  $\leq \log_2 -3 \text{ mm}^{-3}$ ) contribute high in total biovolume (76.84%); whereas larger copepods contribution was high in core-eddy. Normalised Abundance Size Spectra (NASS) slopes varied from -2.45 to -1.02 and their differences were significant between the eddy phases. The NASS slopes were steeper during pre-eddy phase compared to core-eddy and transition phases. The variations in the size diversity, biovolume, NASS slopes and copepods community structure reveals that pre eddy phase contains the small coastal forms; core-eddy includes the mixture of small coastal and larger oceanic and OMZ tolerant forms. Presence of larger oceanic and OMZ tolerant forms in core-eddy indicates their entry through cold-core eddy in the study site. Slopes and intercept of NASS and size diversity suggest that copepods production and trophic efficiency was comparatively high in core-eddy. Slopes and intercepts of NASS captured the copepods composition and production differences between the eddy phases in terms of abundance. Hence, the results of plankton size spectra can be used as a useful tool to predict the plankton food web response in the varying environmental conditions. This study is the first kind of information about copepods size structure and size

spectrum from Indian waters, specifically direct comparative study in various phases of a moving cold-core eddy.

### **Acknowledgement**

The authors thank the Director, CSIR- National Institute of Oceanography, India, for facilities and encouragement. The authors thank the Scientist-in-Charge, CSIR NIO RC Visakhapatnam for encouragement and support. The authors thank the Dr.V.S.N. Murty, Dr. M. Dileep Kumar and Dr.V.V.S.S. Sarma from CSIR, NIO, RC, Visakhapatnam for their constant assistance and initial review of the manuscript. The authors thank all participants and the ship members who extended their help for the successful completion of the SSK 088 cruise. This is NIO contribution XXXX.

### **References**

- Álvarez, E., López-Urrutia, Á., Nogueira, E., Fraga, S., 2011. How to effectively sample the plankton size spectrum? A case study using FlowCAM. *Journal of Plankton Research* 33, 1119-1133.
- Anjusha, A., Jyothibabu, R., Jagadeesan, L., Mohan, A.P., Sudheesh, K., Krishna, K., Ullas, N., Deepak, M.P., 2013. Trophic efficiency of plankton food webs: Observations from the Gulf of Mannar and the Palk Bay, Southeast Coast of India. *Journal of Marine Systems* 115-116, 40-61.
- Blanco, J.M., Echevarría, F., García, C.M., 1994. Dealing with size-spectra: some conceptual and mathematical problems. *Scientia Marina (España)*.
- Brucet, S., Boix, D., López-Flores, R.o., Badosa, A., Quintana, X.D., 2006. Size and species diversity of zooplankton communities in fluctuating Mediterranean salt marshes. *Estuarine, Coastal and Shelf Science* 67, 424-432.
- Clarke, K.R., Gorley, R.N., 2006. *PRIMER(Plymouth Routine In Multivariate Ecological Research) V6:User Manual/Tutorial*. 90
- Conway, D.V.P., White, R.G., Hugues-Dit-Ciles, J., Gallienne, C.P., Robins, D.B., 2003. Guide to the coastal and surface zooplankton of the south-western Indian Ocean. Occasional Publication of the Marine Biological Association 15.
- Fernandes, V., 2008. The effect of semi-permanent eddies on the distribution of mesozooplankton in the central Bay of Bengal. *Journal of Marine Research* 66, 465-488.
- Fernandes, V., Ramaiah, N., 2009. Mesozooplankton community in the Bay of Bengal (India): spatial variability during the summer monsoon. *Aquatic Ecology* 43, 951-963.

- Gauns, M., Madhupratap, M., Ramaiah, N., Jyothibabu, R., Fernandes, V., Paul, J.T., Kumar, S.P., 2005. Comparative accounts of biological productivity characteristics and estimates of carbon fluxes in the Arabian Sea and the Bay of Bengal. *Deep-Sea Research Part II: Topical Studies in Oceanography* 52, 2003-2017.
- Gillooly, J.F., Brown, J.H., West, G.B., Savage, V.M., Charnov, E.L., 2001. Effects of size and temperature on metabolic rate. *Science* 293, 2248-2251.
- Grasshoff, K., 1983. *Methods of Seawater Analysis*, in: Grasshoff, K., Ehrhardt, M., Kremling, K., (Ed.). Weinheim, Verlag Chemie p. 419.
- Jagadeesan, L., Jyothibabu, R., Anjusha, A., Mohan, A.P., Madhu, N.V., Muraleedharan, K.R., Sudheesh, K., 2013. Ocean currents structuring the mesozooplankton in the Gulf of Mannar and the Palk Bay, southeast coast of India. *Progress in Oceanography* 110, 27-48.
- Jagadeesan, L., Jyothibabu, R., Arunpandi, N., Karnan, C., Balachandran, K.K., 2017a. Dominance of coastal upwelling over Mud Bank in shaping the mesozooplankton along the southwest coast of India during the Southwest Monsoon. *Progress in Oceanography* 156, 252-275.
- Jagadeesan, L., Jyothibabu, R., Arunpandi, N., Anjusha, A., Parthasarathi, S., Pandiyarajan, R.S., 2017b. Feeding preference and daily ration of 12 dominant copepods on mono and mixed diets of phytoplankton, rotifers, and detritus in a tropical coastal water. *Environmental monitoring and assessment* 189, 503.
- Jagadeesan, L., Kumar, G.S., Rao, D.N., Srinivas, T.N.R., 2019. Role of eddies in structuring the mesozooplankton composition in coastal waters of the western Bay of Bengal. *Ecological Indicators* 105, 137-155.
- Jyothibabu, R., Madhu, N.V., Maheswaran, P.A., Jayalakshmy, K.V., Nair, K.K.C., Achuthankutty, C.T., 2008a. Seasonal variation of microzooplankton (20  $\mu\text{m}$  – 200  $\mu\text{m}$ ) and its possible implications on the vertical carbon flux in the western Bay of Bengal. *Continental Shelf Research* 28, 737-755.
- Jyothibabu, R., Asha Devi, C.R., Madhu, N.V., Sabu, P., Jayalakshmy, K.V., Josia Jacob, Habeebrehman, H., Prabhakaran, M.P., Balasubramanian, T., Nair, K.K.C., 2008b. The response of microzooplankton (20–200  $\mu\text{m}$ ) to coastal upwelling and summer stratification in the southeastern Arabian Sea. *Continental Shelf Research* 28, 653–671.
- Jyothibabu, R., Vinayachandran, P.N., Madhu, N.V., Robin, R.S., Karnan, C., Jagadeesan, L., Anjusha, A., 2015. Phytoplankton size structure in the southern Bay of Bengal modified by the Summer Monsoon Current and associated eddies: Implications on the vertical biogenic flux. *Journal of Marine Systems* 143, 98-119.
- Kasturirangan, L.R., 1963. A key for the identification of the more common planktonic Copepoda of the Indian coastal waters, Publication No.2. Indian National Committee on Oceanic Research, 1- 87.
- Ke, Z., Tan, Y., Huang, L., Liu, J., Liu, H., 2018. Community structure and biovolume size spectra of mesozooplankton in the Pearl River estuary. *Aquatic ecosystem health & management* 21, 30-40.
- Le Bourg, B., Cornet-Barthaux, V.r., Pagano, M., Blanchot, J., 2015. FlowCAM as a tool for studying small (80-1000  $\mu\text{m}$ ) metazooplankton communities. *Journal of Plankton Research* 37, 666-670.

- Leps, J., Smilauer, P.S., 2003. Multivariate analysis of ecological data using CANOCA. Cambridge university press, Cambridge, UK.
- Mackas, D.L., Tsurumi, M., Galbraith, M.D., Yelland, D.R., 2005. Zooplankton distribution and dynamics in a North Pacific Eddy of coastal origin: II. Mechanisms of eddy colonisation by and retention of offshore species. *Deep-Sea Research Part II: Topical Studies in Oceanography* 52, 1011-1035.
- Madhu, N.V., Jyothibabu, R., Maheswaran, P.A., John Gerson, V., Gopalakrishnan, T.C., Nair, K.K.C., 2006. Lack of seasonality in phytoplankton standing stock (chlorophyll a) and production in the western Bay of Bengal. *Continental Shelf Research* 26, 1868-1883.
- Madhupratap, M., Haridas, P., Ramaiah, N., Achuthankutty, C.T., 1992. Zooplankton of the southwest coast of India: abundance, composition, temporal and spatial variability in 1987, in: Desai, B.N. (Ed.), *Oceanography of Indian Ocean*, Oxford & IBH, New Delhi, pp. 99-112.
- Madhupratap, M., Gopalakrishnan, T.C., Haridas, P., Nair, K.K.C., Aravindakshan, P.N., Padmavati, G., Paul, S., 1996. Lack of seasonal and geographic variation in mesozooplankton biomass in the Arabian Sea and its structure in the mixed layer. *Current Science* 71, 863-868.
- Madhupratap, M., Gopalakrishnan, T.C., Haridas, P., Nair, K.K.C., 2001. Mesozooplankton biomass, composition and distribution in the Arabian Sea during the fall intermonsoon: implications of oxygen gradients. *Deep-Sea Research Part II: Topical Studies in Oceanography* 48, 1345-1368.
- Mahadevan, A., 2014. The impact of submesoscale physics on primary productivity of plankton. *Annual review of Marine Science* 8, 161-184.
- Marcolin, d.R., Schultes, C., Sabine Jackson, A., G., Lopes, R.M., 2013. Plankton and seston size spectra estimated by the LOPC and ZooScan in the Abrolhos Bank ecosystem (SE Atlantic). *Continental Shelf Research* 70, 74-87.
- Platt, T., 1978. The structure of pelagic marine ecosystems. *Rpp. P.-v. Cons. int. Explor. Mer.* 173, 60-65.
- Postel, L., Fock, H., Hagen, W., 2000. Biomass and abundance, ICES Zooplankton Methodology manual. Harris R.P., Wiebe. P.H., Leiz. J., Skjoldal et al, editors. Academic Press, 193 – 213.
- Prasanna Kumar, S., Muraleedharan, P.M., Prasad, T.G., Gauns, M., Ramaiah, N., de Souza, S.N., Sardesai, S., Madhupratap, M., 2002. Why is the Bay of Bengal less productive during summer monsoon compared to the Arabian Sea? *Geophysical Research Letters* 29, 88-81-88-84.
- Prasanna Kumar, S., Nuncio, M., Narvekar, J., Kumar, A., Sardesai, S., De Souza, S.N., Gauns, M., Ramaiah, N., Madhupratap, M., 2004. Are eddies nature's trigger to enhance biological productivity in the Bay of Bengal? *Geophysical Research Letters* 31.
- Prasanna Kumar, S., Nuncio, M., Ramaiah, N., Sardesai, S., Narvekar, J., Fernandes, V., Paul, J.T., 2007. Eddy-mediated biological productivity in the Bay of Bengal during fall and spring intermonsoons. *Deep Sea Research Part I: Oceanographic Research Papers* 54, 1619-1640.
- Rakesh, M., Raman, A.V., Sudarsan, D., 2006. Discriminating zooplankton assemblages in neritic and oceanic waters: a case for the northeast coast of India, Bay of Bengal. *Marine Environmental Research* 61, 93-109.

- Rakesh, M., Raman, A.V., Kalavati, C., Subramanian, B.R., Sharma, V.S., SunithaBabu, E., Sateesh, N., 2008. Zooplankton community structure across an eddy- generated upwelling band close to a tropical bay-mangrove ecosystem. *Marine Biology* 154, 953-972.
- Sarma, V., Jagadeesan, L., Dalabehera, H.B., Rao, D.N., Kumar, G.S., Durgadevi, D.S., Yadav, K., Behera, S., Priya, M.M.R., 2018. Role of eddies on intensity of oxygen minimum zone in the Bay of Bengal. *Continental Shelf Research* 168, 48-53.
- Shankar, D., Vinayachandran, P.N., Unnikrishnan, A.S., 2002. The monsoon currents in the north Indian Ocean. *Progress in Oceanography* 52, 63-120.
- Shannon, C.E., Weaver, W., 1963. *The mathematical theory of communication*. 1949. Urbana, IL: University of Illinois Press.
- Sheldon, R.W., Prakash, A., Sutcliffe Jr, W., 1972. The size distribution of the particles in the Ocean. *Limnology and Oceanography* 17, 327-340.
- Shetye, S.R., Gouveia, A.D., Shenoi, S.S.C., Sundar, D., Michael, G.S., Nampoothiri, G., 1993. The western boundary current of the seasonal subtropical gyre in the Bay of Bengal. *Journal of Geophysical Research: Oceans* 98, 945-954.
- Shetye, S.R., Gouveia, A.D., Shankar, D., Shenoi, S.S.C., Vinayachandran, P.N., Sundar, D., Michael, G.S., Nampoothiri, G., 1996. Hydrography and circulation in the western Bay of Bengal during the northeast monsoon. *Journal of Geophysical Research: Oceans* 101, 14011-14025.
- Sieracki, C.K., Sieracki, M.E., Yentsch, C.S., 1998. An imaging-in-flow system for automated analysis of marine microplankton. *Marine Ecology Progress Series* 168, 285-296.
- Silvert, W., Platt, T., 1978. Energy flux in the pelagic ecosystem: a time dependent equation. *Limnology and oceanography* 23, 813-816.
- Taucher, J., Haunost, M., Boxhammer, T., Bach, L.T., AlguerÃ³-MuÃ±iz, M., Riebesell, U., 2017. Influence of ocean acidification on plankton community structure during a winter-to-summer succession: An imaging approach indicates that copepods can benefit from elevated CO<sub>2</sub> via indirect food web effects. *PloS one* 12, e0169737.
- Turner, J.T., 1986. Zooplankton Feeding Ecology: Contents of Fecal Pellets of the Cyclopoid Copepods *Oncaea venusta*, *Corycaeus amazonicus*, *Oithona plumifera*, and *O. simplex* from the Northern Gulf of Mexico. *Marine Ecology* 7, 289-302.
- Viñas, M.D., Diovisalvi, N.R., Cepeda, G.D., 2010. Individual biovolume of some dominant copepod species in coastal waters off Buenos Aires Province, Argentina sea. *Brazilian Journal of Oceanography* 58, 177-181.
- Visser, A.W., Fiksen, Ø., 2013. Optimal foraging in marine ecosystem models: selectivity, profitability and switching. *Marine Ecology Progress Series* 473, 91-101.
- Wong, E., Sastri, A.R., Lin, F.-S., Hsieh, C.-h., 2017. Modified FlowCAM procedure for quantifying size distribution of zooplankton with sample recycling capacity. *PloS one* 12, e0175235.
- Woodward, G., Ebenman, B., Emmerson, M., Montoya, J.M., Olesen, J.M., Valido, A., Warren, P.H., 2005. Body size in ecological networks. *Trends in ecology & evolution* 20, 402-409.



- Wu, C.-H., Hwang, J.-S., Yang, J.-S., 2004. Diets of three copepods (Poecilostomatoida) in the southern Taiwan Strait. *Zool Stud* 43, 388-392.
- Yang, G.M., He, D.H., Wang, C.S., Miao, Y.T., Yu, H.H., 1999. Study on the biological oceanography characteristics of planktonic copepods in the waters north of Taiwan, II. Community characteristics. *Acta Oceanol. Sin* 21, 72-80.
- Ye, L., Chang, C.Y., Garc a Comas, C., Gong, G.C., Hsieh, C.h., 2013. Increasing zooplankton size diversity enhances the strength of top-down control on phytoplankton through diet niche partitioning. *Journal of Animal Ecology* 82, 1052-1061.
- Zar, J.H., 1999. *Biostatistical analysis* (4th ed.). Prentice-Hall, Upper Saddle River.
- Zhou, L., Huang, L., Tan, Y., Lian, X., Li, K., 2015. Size-based analysis of a zooplankton community under the influence of the Pearl River plume and coastal upwelling in the northeastern South China Sea. *Marine Biology Research* 11, 168-179.
- Zhou, M., 2006. What determines the slope of a plankton biomass spectrum? *Journal of Plankton Research* 28, 437-448.
- Zhou, M., Huntley, M.E., 1997. Population dynamics theory of plankton based on biomass spectra. *Marine Ecology Progress Series* 159, 61-73.
- Zhou, M., Tande, K.S., Zhu, Y., Basedow, S.N., 2009. Productivity, trophic levels and size spectra of zooplankton in northern Norwegian shelf regions. *Deep Sea Research Part II: Topical Studies in Oceanography* 56, 1934-1944.

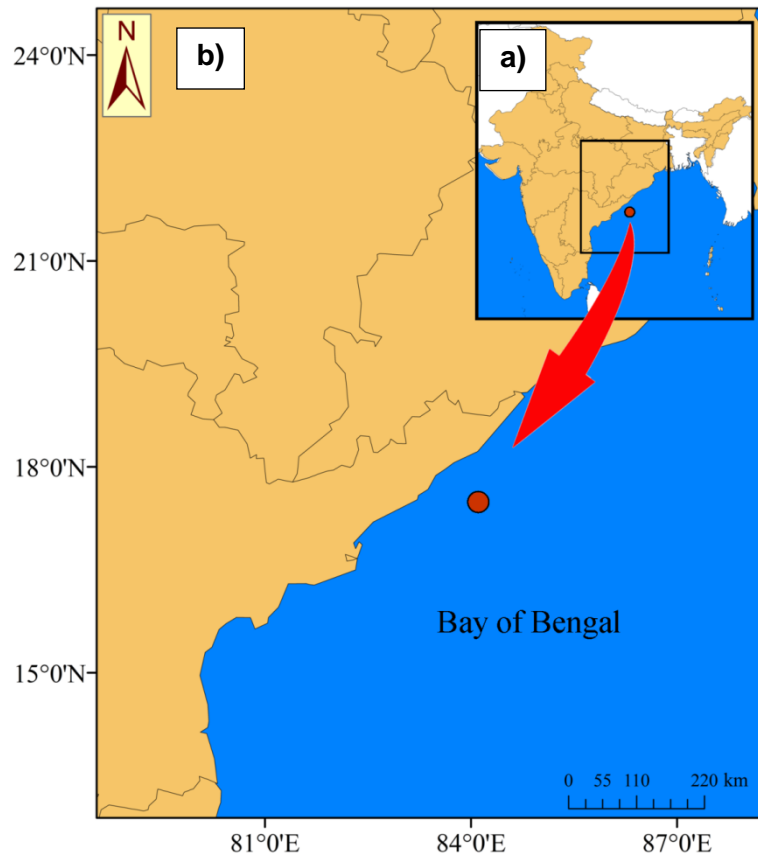


**Figure – 1** - Time series study location of the present study (off Bheemunipatnam – red rot). (a) India with state boundaries (insertion) and the present study area (red dot), and (b) an enlargement of the study area (Square area). The study location is situated ~ 80 Km away from the shore and located 50 km north from the Off Visakhapatnam. Depth of the study site was 110m.

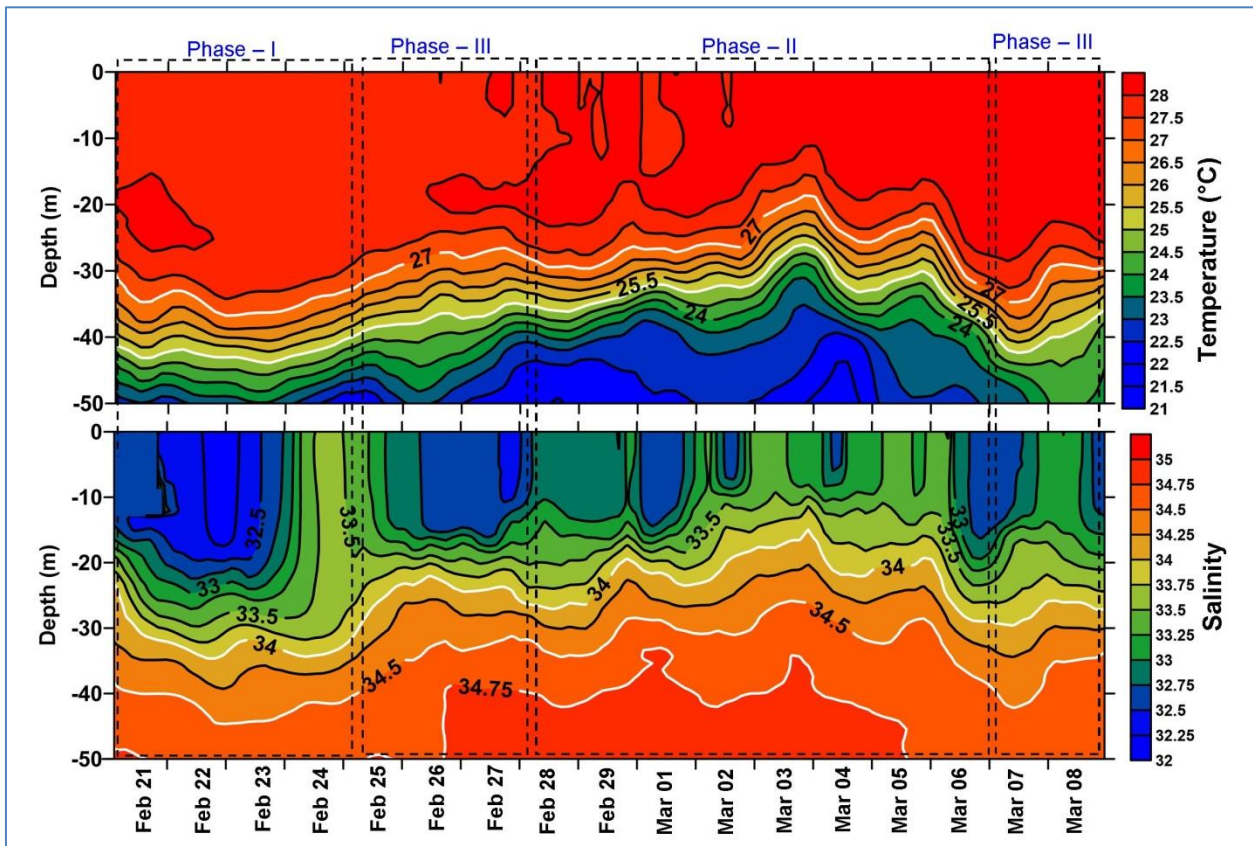


**Figure 2.** Vertical distribution of (a) temperature (in°C) and (b) salinity from February 21 to March 8 and the depth interval from 0 to 50 m at the study location. Isotherms of 25°C and 27°C and isohalines of 34 and 34.5 and 34.75 exhibit the shoaling from 25<sup>th</sup> February to 6<sup>th</sup> March. Black dotted lines represent the various phases of the sampling period (additional information, please see figure 3).

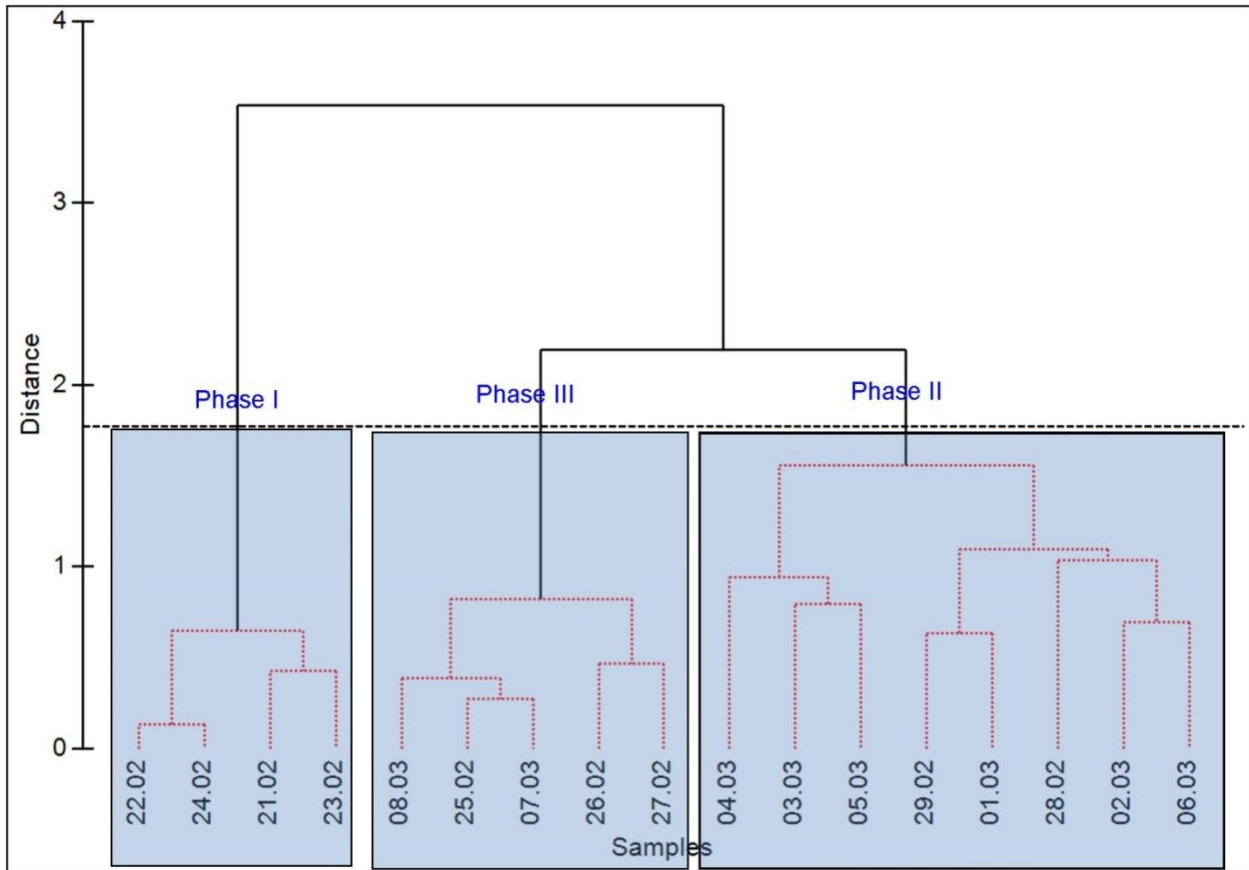


**Figure 3 - a)** Euclidean distance matrix and group average linkage method of cluster and SIMPROF overlaid (Similarity Profile) combined results are presented in the form of the dendrogram. The dendrogram visualises the delineation of sampling days based on the similarities of hydrographical parameters (salinity, temperature) in various depth layers viz., surface, 10, 20, 25, 30, 40 and 50m depth layers. In the dendrogram, solid black lines show the statistically significant segregations of the groups and red dashed lines indicate groups of samples not separated (at  $P < 0.05$ ) by SIMPROF. Sampling days 21<sup>st</sup> February to 24<sup>th</sup> February grouped as cluster I (phase I – pre-eddy); 28<sup>th</sup> February to 6<sup>th</sup> March grouped as cluster II (phase II – core-eddy) and 25<sup>th</sup> February to 27<sup>th</sup> February and 7<sup>th</sup> and 8<sup>th</sup> March were grouped as cluster III (phase III - transition phase). Cluster III located between cluster I and II indicate the intermittent between the pre-eddy and core-eddy.

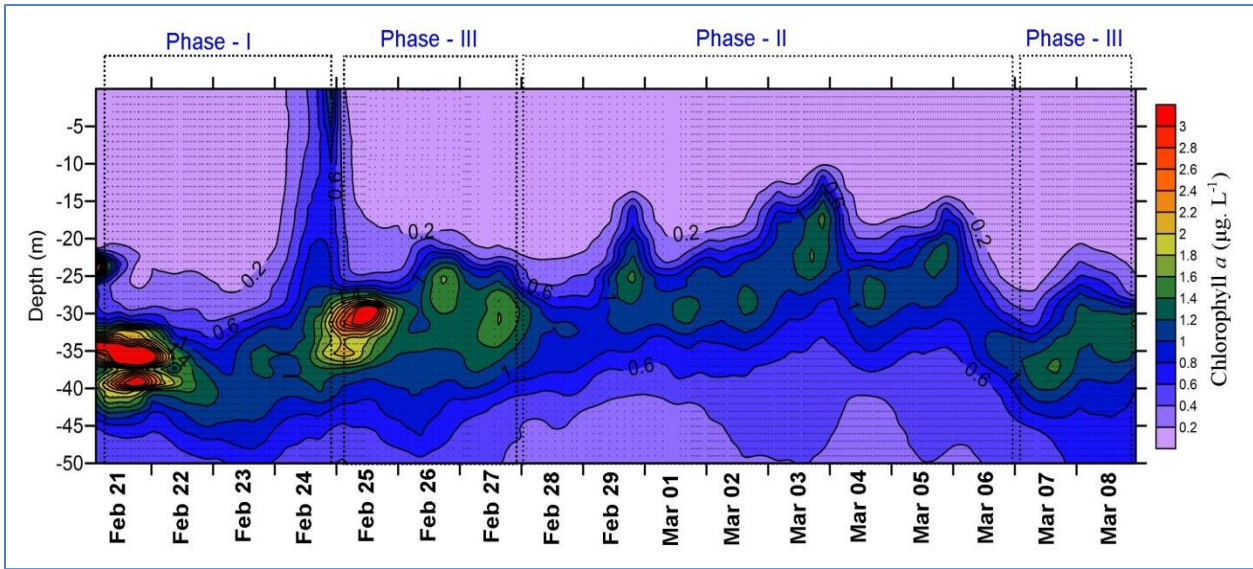


**Figure 4-** Variations of Chlorophyll *a* in the time period from February 21 to March 8 measured at the study location: Temporal change of the Chlorophyll *a* ( $\mu\text{g/L}$ ) in the depth interval from 0 to 50 m, DCM layer becomes shallower from  $\sim 40\text{m}$  of pre-eddy period (February 21 to February 24) to  $\sim 20\text{ m}$  of core-eddy phase was quite evident.

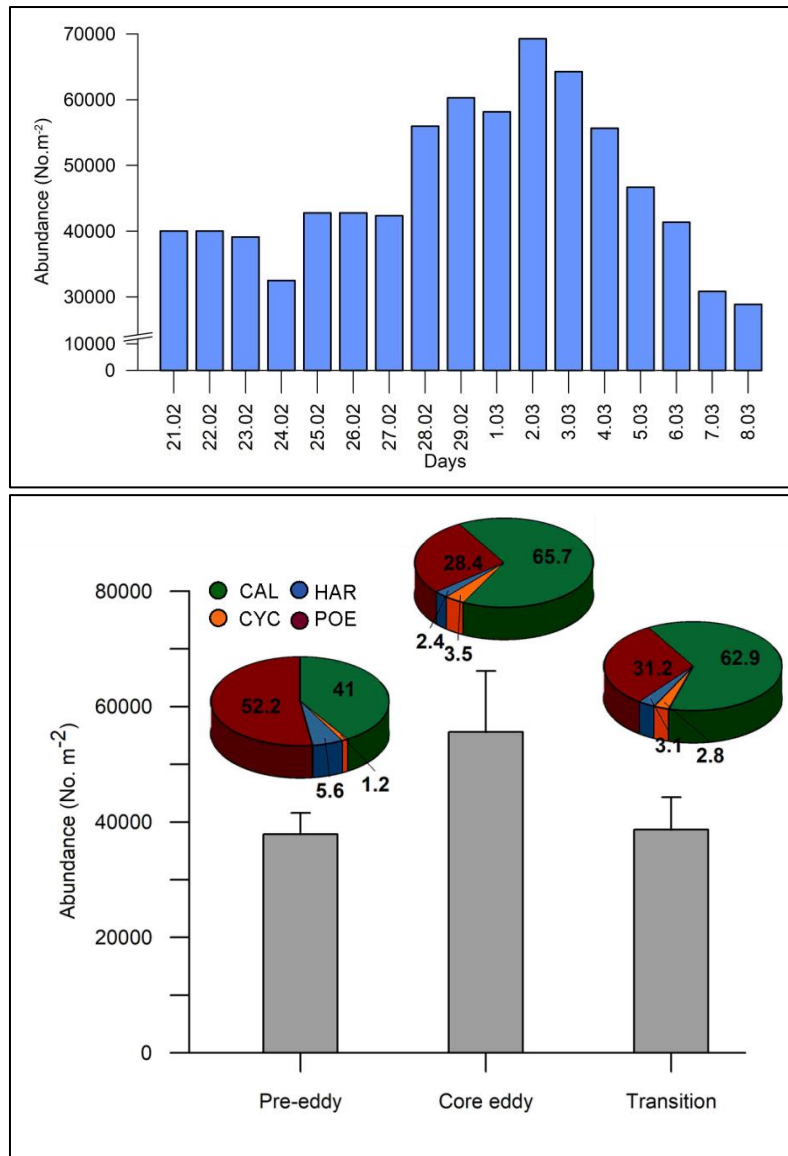


**Figure 5** - Copepods abundance (0-100m) and contribution of various copepods orders in total abundance during the study period from February 21 to March 08 at the study location (a) Abundances of copepods (No.m<sup>-2</sup>) and represented values are the daily mean and SD values of the particular day (b). Copepod abundance (Mean and SD of the specific phase) and contribution of four copepods orders to the total copepods in three eddy phases (Pie chart). CAL – Calanoids; CYC- Cyclopods – Cyclopoida; POE- Poecilostomatoida\*; (POE); HAR- Harpacticoida. \*Presently Poecilostomatoida is merged with the cyclopoids. For representing the actual role of the family of Oncaeade and Corycaediae (previously belongs in order Poecilostomatoida) presented as per the earlier classification as Poecilostomatoida.

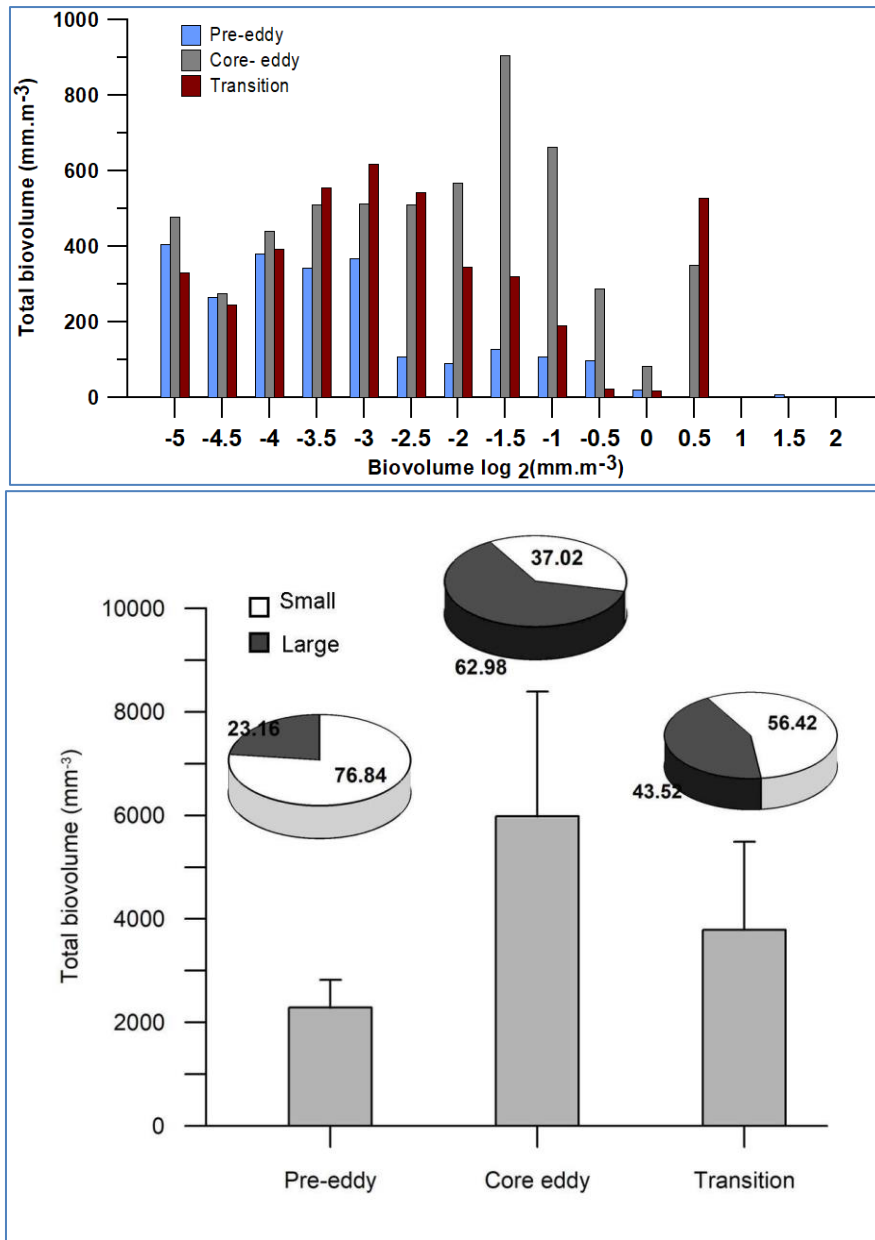


**Figure 6** (a) Temporal variation of copepod biovolume (mm. m<sup>-3</sup>) in various size classes (Bar charts). \*Biovolume size classes are in log<sub>2</sub> scale. Data: Mean biovolume in each size classes and small and larger copepods (pie chart) proportions (Percentages) in the total biovolume during pre-eddy (phase I), core-eddy (phase II) and transition (phase III). Total biovolume with means (grey bars) and standard deviations (error bars) of a specific phase. Data = total copepod biovolume in 0-100m; Two size division: small (Biovolume <0.13 mm<sup>-3</sup>) and Large (>0.13 mm<sup>-3</sup>).

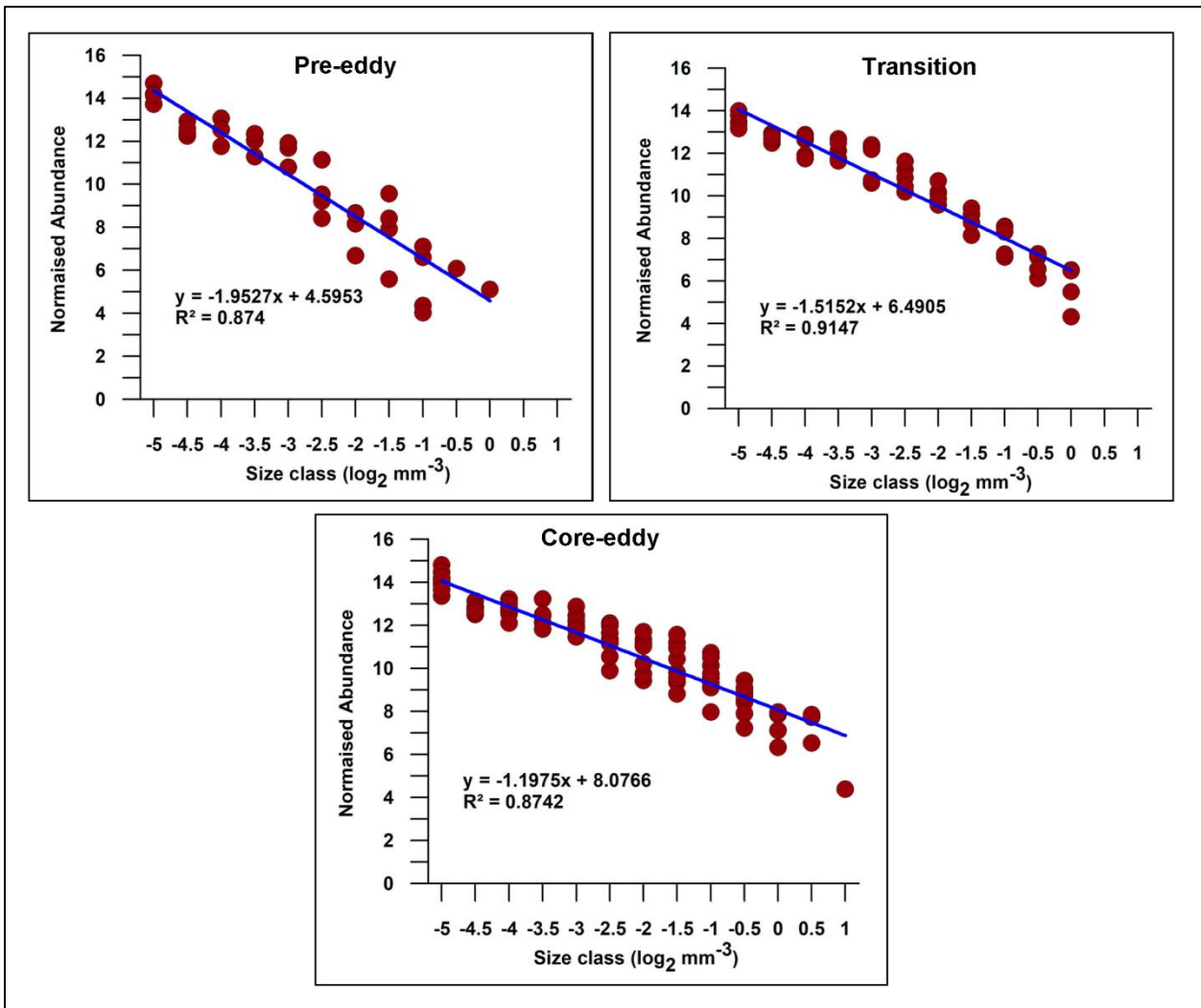


**Figure – 7** - Normalised Abundance Size Spectrum (NASS) of copepods in various eddy phases. Data: Normalised abundance of copepod in each size classes of the sampling days in particular eddy phases (pre-eddy- 21<sup>st</sup> February to 24<sup>th</sup> February; Core eddy - 28th February to 6<sup>th</sup> March; transition phase - 25<sup>th</sup> February to 27<sup>th</sup> February and 7<sup>th</sup> and 8<sup>th</sup> March) are plotted in log-log scale and fitted with regression model (solid blue lines). The slope of the pre eddy phase was steeper (-1.95) and shallower (-1.198) in core-eddy phase.



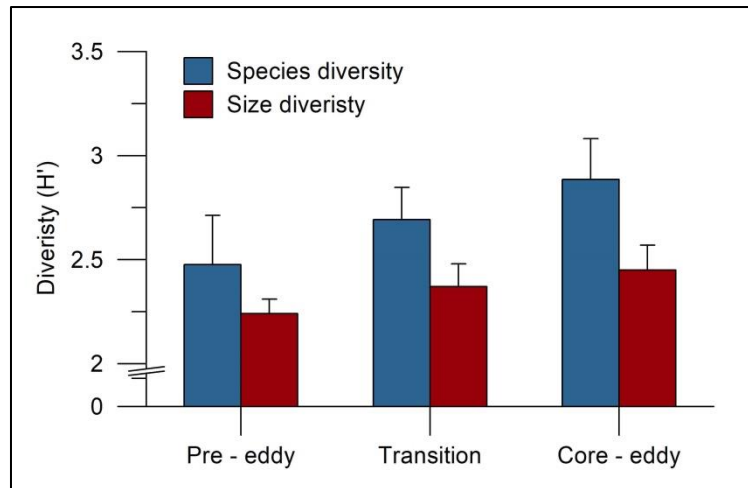


**Figure – 8.** Species diversity and size diversity of copepods in various phases of the cold-core eddy. Both the diversity indices were high in the core-eddy compared to Pre eddy. Data: Species diversity was calculated using the copepods abundance data of each sampling days, from that eddy phases mean (Bar)  $\pm$  SD (error bars) calculated and presented; Size diversity was calculated using the 15 biovolume size classes of copepods in each sampling day and that eddy phases mean  $\pm$  SD was calculated and presented.

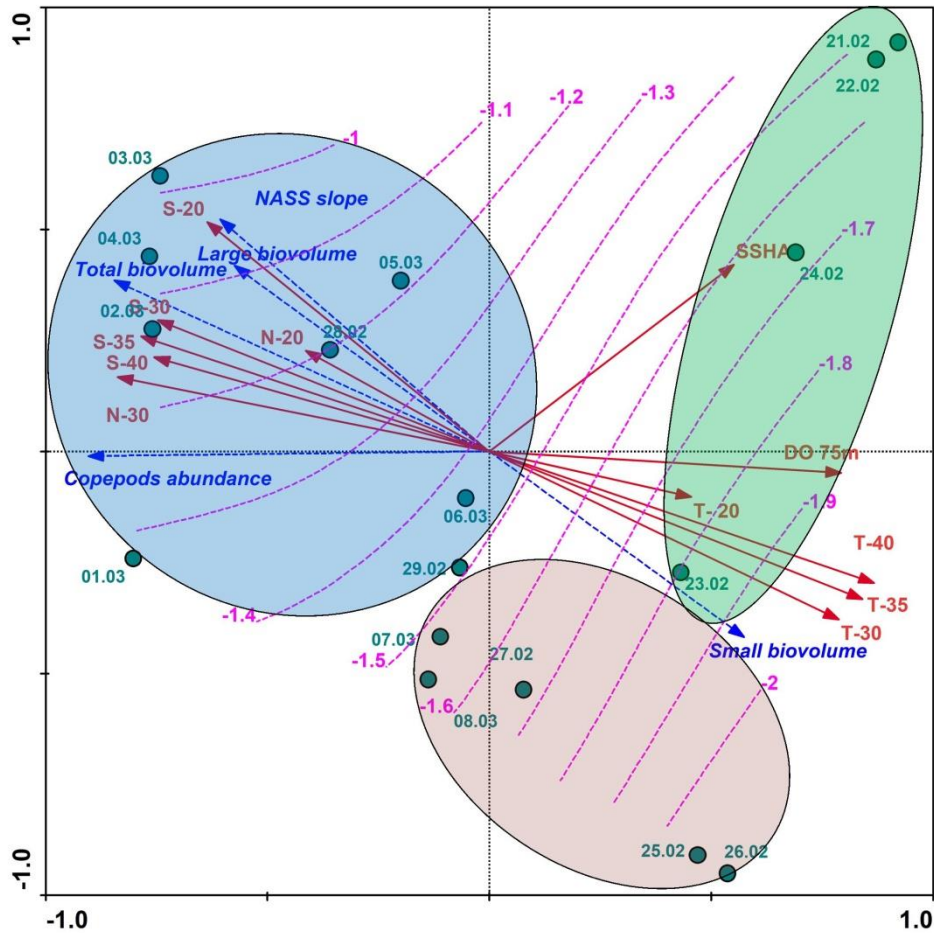


**Figure 9** - Redundancy analysis (RDA) triplot of the relationship between the copepods abundance, biovolume, contribution of smaller and larger copepods in biovolume and Normalised abundance. Size spectra slopes (Blue dotted arrows) and the environmental parameters (Red arrows). Sampling days were represented by the green circles. Daily mean values of hydrographical parameters and copepods abundance were used for the creation of RDA triplot. Copepods species abundances and total biovolume ( $\text{Ind.m}^{-2}$ ) was log transformed before the analysis of RDA. For visualising the size structure differences, NASS slopes were attributed as an overlay (pink dotted lines) in the base RDA. For showing the various phases and their characteristic feature, eclipses are drawn and shaded with various colours. The green shaded portions show that the phase I (pre-eddy) characteristics; blue shaded portions show that the Phase II (core-eddy); brown shaded portions show the transition conditions (Phase III). Abbreviations; S-XX indicates the salinity in depth Viz., S-20, S-30, S-35; S-40 indicates the salinity at 20m, 30, 35m and 40m. T-XX indicates the temperature in depth Viz., T-20, T-30, T-35, T-40 indicates Temperature in the depth of 20m, 30m, 35m and 40m. N-20 – Nitrate 20m; N-30 – Nitrate 30m; DO-75m – Dissolved oxygen - 75m; SSHA – Sea surface height anomaly.

Parameter	Phase	Surface	10m	20m	30m	50m	75m	100m
Dissolved oxygen (mg.L <sup>-1</sup> )	pre-eddy	6.09±	6.2 ±	5.81 ±	5.14 ±	3.41 ±	0.83 ±	0.51 ±
		0.36	0.29	0.4	0.99	2.56	0.13	0.04
	core-eddy	6.54 ±	6.36 ±	5.39 ±	2.97 ±	1.23 ±	0.43 ±	0.28 ±
		1.09	0.90	1.27	0.77	0.43	0.17	0.21
	transition	6.71 ±	6.61 ±	6.64 ±	4.99 ±	1.33 ±	0.42 ±	0.41 ±
		0.67	0.61	0.66	1.60	0.44	0.24	0.21
Nitrate (μM)	pre-eddy	0.51 ±	1.19 ±	1.87 ±	3.85 ±	11.69 ±	18.79 ±	21.03 ±
		0.19	0.70	0.89	1.47	4.85	4.49	2.55
	core-eddy	0.45 ±	1.12 ±	3.12 ±	6.90 ±	16.08 ±	15.46 ±	18.74 ±
		0.08	0.41	0.40	1.29	2.18	3.19	4.49
	transition	0.63 ±	0.87 ±	2.39 ±	4.88 ±	15.09 ±	18.60 ±	20.62 ±
		0.15	0.45	1.09	1.62	3.25	4.18	3.52
Phosphate (μM)	pre-eddy	0.45 ±	0.54 ±	0.61 ±	0.97 ±	1.86 ±	2.21 ±	2.36 ±
		0.09	0.05	0.09	0.18	0.40	0.23	0.19
	core-eddy	0.61 ±	0.56 ±	0.71 ±	1.19 ±	1.82 ±	1.95 ±	2.24 ±
		0.28	0.16	0.17	0.25	0.27	0.19	0.15
	transition	0.49 ±	0.48 ±	0.49 ±	0.83 ±	1.76 ±	2.08 ±	2.21 ±
		0.19	0.09	0.10	0.19	0.17	0.11	0.11
Silicate	pre-eddy	4.05 ±	4.25 ±	4.27 ±	6.11 ±	18.45 ±	23.63 ±	26.73 ±
		1.49	1.76	1.43	3.48	2.41	2.57	2.96

( $\mu\text{M}$ )	core-	$4.91 \pm$	$5.78 \pm$	$6.56 \pm$	$10.16 \pm$	$18.86 \pm$	$19.77 \pm$	$26.61 \pm$
	eddy	0.43	1.62	2.17	3.21	1.65	3.02	1.97
	transition	$4.05 \pm$	$3.89 \pm$	$4.56 \pm$	$6.99 \pm$	$15.96 \pm$	$21.95 \pm$	$24.01 \pm$
		1.16	1.58	2.44	2.02	0.99	2.12	1.94

---

**Table -1-** Vertical distribution of dissolved oxygen and nutrients (mean  $\pm$  standard deviation) in various eddy phases during the study period February 21 - March 08 in the study site. Pre-eddy, core-eddy and transition grouping of sampling day according to Figure 5. Total number of number of samples = 136; N=32 in Pre eddy ; N= 40 in transition and N= 64 in core-eddy.

Dominant species	pre-eddy	transition	core-eddy
<i>Acrocalanus</i> sp.	0.125 (0.032 ± 0.012)	0.178 (0.045 ± 0.016)	0.112 (0.061 ± 0.011)
<i>Calocalanus pavo</i>	0.024 (0.034 ± 0.016)	0.027 (0.051 ± 0.021)	0.029 (0.062 ± 0.051)
<i>Canthocalanus pauper</i>	-	0.021 (0.098 ± 0.015)	0.029 (0.11 ± 0.07)
<i>Centropages calaninus</i>	0.029 (0.09 ± 0.021)	-	-
<i>Corycaeus danae</i>	0.070 (0.024 ± 0.014)	0.035 (0.026 ± 0.012)	0.038 (0.025 ± 0.04)
<i>Eucalanus elongatus</i>	0.025 (0.34 ± 0.041)	0.030 (0.46 ± 0.06)	0.067 (0.51 ± 0.12)
<i>Euterpina acutifrons</i>	0.044 (0.032 ± 0.016)	0.021 (0.035 ± 0.012)	-
<i>Farranula gibbula</i>	0.039 (0.024 ± 0.015)	0.043 (0.024 ± 0.009)	0.022 (0.025 ± 0.012)
<i>Oncaea venusta</i>	0.371 (0.031 ± 0.014)	0.201 (0.032 ± 0.013)	0.197 (0.029 ± 0.008)
<i>Paracalanus parvus</i>	0.074 (0.06 ± 0.012)	0.080 (0.08 ± 0.041)	0.083 (0.12 ± 0.05)
<i>Pleuromamma indica</i>	-	0.021 (0.54 ± 0.11)	0.064 (0.64 ± 0.11)
<i>Pseudodiaptomus</i>	-	0.026 (0.32 ± 0.14)	0.021 (0.41 ± 0.06)

*serricaudatus*

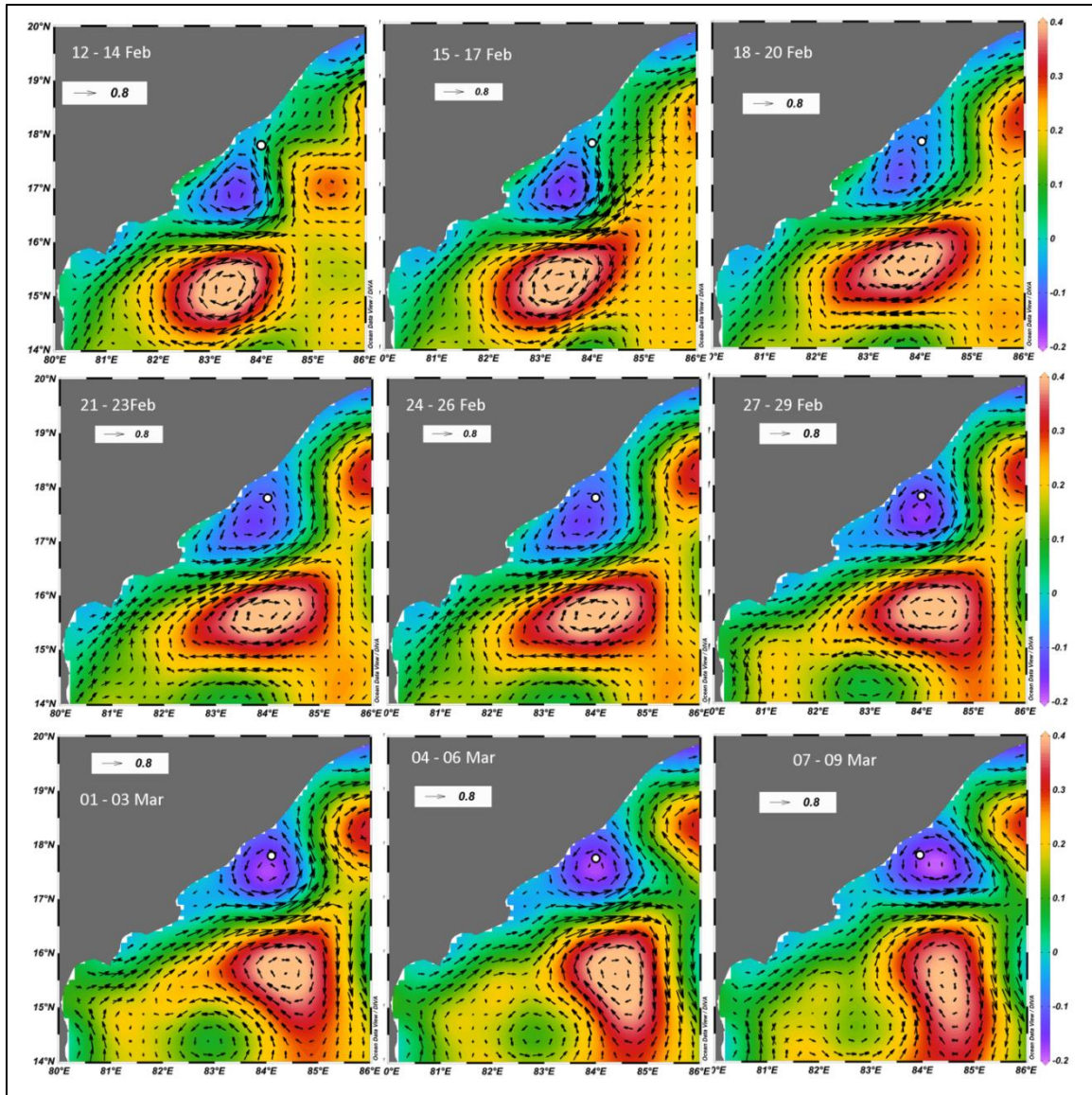
<i>Temora turbinata</i>	-	0.022 (0.16 ± 0.08)	0.037 (0.23 ± 0.08)
<i>Undinula vulgaris</i>	-	0.048 (0.34 ± 0.07)	0.029 (0.41 ± 0.06)

---

**Table – 2** List of the dominant species (dominance index value  $Y_i \geq 0.02$ ) and their dominance values ( $Y_i$ ) and biovolume ( $\text{mm}^{-3}$ ) in various phases of the eddy conditions. – sign represents species are absent or their dominance values are less than 0.02 in that phase.

Sampling date	Slope	Intercept	R <sup>2</sup>	P value
21.02.2016	-2.455	2.263	0.958	<0.01
22.02.2016	-2.254	3.520	0.883	<0.01
23.02.2016	-1.776	5.338	0.960	<0.01
24.02.2016	-1.699	5.922	0.922	<0.01
25.02.2016	-1.392	7.212	0.939	<0.01
26.02.2016	-1.717	5.861	0.934	<0.01
27.02.2016	-1.599	6.477	0.920	<0.01
28.02.2016	-1.145	8.595	0.885	<0.01
29.02.2016	-1.217	7.397	0.928	<0.01
01.03.2016	-1.364	7.620	0.902	<0.01
02.03.2016	-1.065	8.879	0.903	<0.01
03.03.2016	-1.242	8.148	0.936	<0.01
04.03.2016	-1.021	9.050	0.905	<0.01
05.03.2016	-1.300	7.456	0.942	<0.01
06.03.2016	-1.164	7.763	0.919	<0.01
07.03.2016	-1.524	6.149	0.920	<0.01
08.03.2016	-1.354	6.733	0.946	<0.01

**Table 3** – Normalised Abundance Size Spectra (NASS) slope, intercept, R<sup>2</sup> and their significance values of the copepods during the study period. Normalised total abundance of copepods in 15 biovolume size classes are plotted in log-log scale and fitted with a linear regression model to estimate slopes and intercepts of the biovolume abundance.



**Supplementary Figure 1-** Dynamics of the eddy (Sea Surface Height Anomaly- SSHA, and geostrophic currents) during the study period from February 12 to March 09. The geostrophic current flow and SSHA data sets were retrieved from the <http://marine.copernicus.eu/> and plotted in Ocean data view. Vertical Color bars represent values of SSHA, study location (white point) faced the positive SSHA during the 2<sup>nd</sup> week of February (12-15 February) and became negative during the 3<sup>rd</sup> week of February (21-23 February), and it decreased later (green to blue to violet). Positive colour values with the clockwise circulation of the geostrophic currents indicates the warm core eddy and negative SSHA and anticlockwise circulation of the currents represents cold core eddy. The current velocity of the geostrophic currents corresponds with reference arrow and the velocity in m/s.



Parameters	N		Surface	10m	20m	30m	50m	75m	100m
Dissolved oxygen (mg.L-1)	136	F ratio	0.38	0.63	2.33	3.87	14.11	4.78	3.21
		P-value	0.68	0.54	0.10	P<0.05*	P<0.001**	P<0.05*	P<0.05*
Phosphate (µM)	136	F ratio	1.73	1.83	2.14	3.39	5.45	6.18	3.67
		P-value	0.18	0.17	0.12	P<0.05*	P<0.05*	P<0.05*	P<0.05*
Silicate (µM)	136	F ratio	2.00	2.05	3.99	5.83	7.49	7.02	4.02
		P-value	0.14	0.13	P<0.05*	P<0.05*	P<0.05*	P<0.05*	P<0.05*
Nitrate (µM)	136	F ratio	0.031	1.06	2.33	3.24	3.58	8.87	4.54
		P-value	0.97	0.35	0.10	P<0.05*	P<0.05*	P<0.001**	P<0.05*
Chlorophyll <i>a</i> (µg.L <sup>-1</sup> )	408	F ratio	1.64	2.80	36.28	25.52	6.04	4.48	2.17
		P-value	0.195	0.062	P<0.001**	P<0.001**	P<0.001**	P<0.05*	0.115
Mesozooplankton abundance (Ind.m <sup>-2</sup> ) (0-100m)	68	F ratio	9.602						
		P-value	P<0.001**						
Copepods abundance (Ind.m <sup>-2</sup> ) (0-100m)	68	F ratio	7.021						
		P-value	P<0.001**						

**Supplementary Table 1** - ANOVA results comparison of dissolved oxygen, nutrients, Chlorophyll *a*, integrated Chlorophyll *a*, mesozooplankton abundance, copepods abundance, larger predators abundance between eddy phases (pre-eddy, core-eddy and transition). N= number of samples, DF=2, significance \*P<0.05 level, \*\*P<0.001 level.